Eur. Phys. J. B **37**, 143–148 (2004)
DOI: 10.1140/epjb/e2004-00040-2

THE EUROPEAN PHYSICAL JOURNAL B

Vibrational properties of C_{20}-based solids

I. Spagnolatti, A. Mussi, M. Bernasconi[a], and G. Benedek

Dipartimento di Scienza dei Materiali and Istituto Nazionale per la Fisica della Materia, Università degli Studi di Milano-Bicocca, Via Cozzi 53, 20125 Milano, Italy

Received 29 September 2003
Published online 15 March 2004 –

Abstract. The phonon dispersion relations and IR spectrum of a C_{20}-based solid recently identified experimentally [Iqbal et al., Eur. Phys. J. B **31**, 509 (2003)] have been computed by density functional perturbation theory. Other competitive structures made by assembling C_{20} clusters have been considered as well. In particular, we have computed the structure and the Raman spectra of two-dimensional polymeric phases of hydrogenated C_{20} clusters which might be formed under different synthesis conditions. Fingerprints of the different phases have been identified in the vibrational spectra which could be used in the experimental search of C_{20}-based solids.

PACS. 61.48.+c Fullerenes and fullerene-related materials – 63.20.-e Phonons in crystal lattices – 78.30.-j Infrared and Raman spectra

1 Introduction

The report on the synthesis of the dodecahedral C_{20} cluster in the gas phase from $C_{20}H_{20}$ precursors [1] encouraged recent research on the properties of the smallest fullerenes [2–4]. Due to the increase of the electron-phonon coupling with increasing curvature of the graphenic cage, the solid phases of the small fullerenes (C_{36} [5], C_{28} [6], C_{20} [3,4,7]) have been suggested to be good candidates for high-T_c superconductors. In this respect, the C_{20} cluster is the most interesting, being the fullerene with the highest curvature. Experimental evidence on the synthesis of the solid form of the C_{20} cluster has been recently provided as well [2]. The new phase has been identified in a diamond-like amorphous film deposited by ultraviolet laser ablation of polycrystalline diamond onto a nickel substrate and in a benzene atmosphere [2]. Electron diffraction, microRaman, and mass spectroscopy measurements combined with ab initio calculations suggested the presence of a crystal with face-centered-cubic symmetry and C_{20} clusters as building blocks [2]. Unlike C_{60}, and more similarly to the proposed solid phase of C_{36} [5], the C_{20}-based crystal is not bound by van der Waals forces, but is instead stabilized by linking the C_{20} cages (sitting on the fcc lattice) with bridging carbon atoms at the tetrahedral interstitial sites. This leads to an fcc crystal with 22 atoms per unit cell (fcc-C_{22}) [2]. Ab initio calculations have shown that fcc-C_{22} can be turned into a metallic system with a large electron-phonon coupling constant ($\lambda = 1.12$) by doping with alkali metals (Li, Na) [3,8]. Another C_{20}-based solid has also been predicted on the only basis of ab initio calculations [4,9], but its structure turned out to be incompatible with the experimental data of reference [2]. This latter C_{20}-based crystal can be seen as originated from the two-dimensional polymerization of C_{20} clusters still on an fcc lattice. The polymerization takes place via [2+2] cycloaddition reaction leading to a 2D polymer similar to the tetragonal phase of polymeric C_{60} [10]. The 2D polymeric planes are further bonded each other via additional intercage covalent bonds leading to a body-centered-orthorombic lattice with a C_{20} cage per unit cell (bco-C_{20} [2,4]). Although inconsistent with the experimental data on the C_{20}-based solid of reference [2], this latter structure has a cohesive energy close to that of fcc-C_{22} and it might thus be synthesized under different experimental conditions.

In this paper we investigate further the properties of fcc-C_{22} and bco-C_{20} crystals by reporting the ab initio calculations of phonon dispersion relations and IR spectrum of fcc-C_{22} and of the Raman spectra of hydrogenated forms of bco-C_{20} which could be formed by assembling partially hydrogenated C_{20} precursors. The calculations provide a prediction on the vibrational properties of these new systems which can aid their experimental identification. The calculations are based on density functional theory in the local density approximation. Computational details are given in Section 2; vibrational properties of fcc-C_{22} and hydrogenated bco-C_{20} phases are reported in Sections 3 and 4, respectively. Section 5 is devoted to discussion and conclusions.

2 Computational details

The calculations are performed within density functional theory in the local density approximation as implemented

[a] e-mail: marco.bernasconi@unimib.it

in the codes PWSCF and PHONONS [11,12]. Norm-conserving pseudopotentials and plane waves expansion of Kohn-Sham orbitals up to a kinetic cutoff of 40 Ry have been used. Phonon dispersion relations, effective charges and dielectric constant (ϵ_∞) of fcc-C_{22} have been computed within density functional perturbation theory [11]. Integration over the electronic states in the Brillouin Zone (BZ) is performed on a 2×2×2 Monkhorst-Pack (MP) mesh [13]. The dynamical matrix of fcc-C_{22} has been computed on a $6\times6\times6$ grid in **q**-space. A Fourier interpolation technique provided the dynamical matrix at the other points of the BZ [11]. The IR spectrum of fcc-C_{22} is obtained from the imaginary part of the dielectric function (the dielectric tensor reducing to a scalar function for a cubic system) given in terms of ab initio phonon polarization vectors η and effective charges **Z** as

$$\epsilon_2(\omega) = \frac{4\pi^2}{3V}\sum_{j,\alpha}\frac{1}{2\omega_j}\Big|\sum_{\kappa,\beta} Z_{\alpha\beta}(\kappa)\eta_{\beta,j}(\kappa)\Big|^2\delta(\omega-\omega_j), \quad (1)$$

where V is the unit cell volume, α and β are Cartesian indices, and κ and j run over atoms in the unit cell and phonons at the Γ-point, respectively. The δ-function in (1) is replaced by a Gaussian function with variance $\sigma = 5$ cm^{-1}. The geometry of isolated hydrogenated C_{20} clusters and of hydrogenated bco-C_{20} crystals have been optimized by Car-Parrinello simulated annealing [14] as implemented in the code CPMD [15]. A time step of 0.12 fs and a fictitious electronic mass of 800 a.u. have been used. Integration of BZ has been restricted to the Γ point in the Car-Parrinello dynamics. Only phonons at the Γ point have been computed for the hydrogenated bco-C_{20} solids. In this latter case, the dynamical matrix has been obtained from finite differences of the forces for finite atomic displacements. The Raman spectra of the hydrogenated bco-C_{20} solids have been calculated from ab initio phonons and empirical polarizability coefficients within the bond polarizability model [16] (BPM). Different BPM coefficients have been used for C=C short double bonds (with length < 1.36 Å), other C-C bonds (with length 1.43−1.58 Å) and C-H bonds as given in reference [16].

3 Vibrational properties of fcc-C_{22}

The crystal structure of fcc-C_{22} (space group Fm$\bar{3}$) is shown in Figure 1. Eight atoms out of twenty of the cage (atoms B in Fig. 1) and the interstitial carbon atoms (A) are sp^3 hybridized. The other twelve atoms of the cage (C) are sp^2 hybridized forming C=C ethylenic bonds. There are three bond lengths in the crystal: the single sp^3-like $B-C$ bond in the pentagonal ring (1.531 Å), the C=C ethylenic-like bond (1.346 Å) long and the single sp^3-like bond between a cage (equivalent to B) and an interstitial atom (A) (1.517 Å). The calculated phonon dispersion relations are reported in Figure 2. The uppermost flat bands correspond to the stretching modes of the ethylenic dimers of the cage. Frequency and symmetry of the Γ-point phonons are given in Table 1.

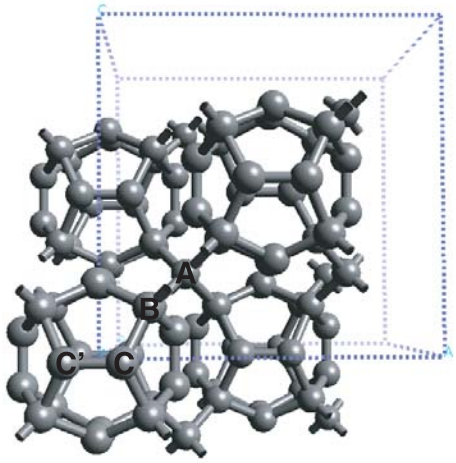

Fig. 1. The face-centered-cubic structure of the fcc-C_{22} crystal. The conventional unit cell with four formula units is shown. The crystal belongs to the Fm$\bar{3}$ space group. The coordinates of the three independent atoms (A, B, C) in units of the lattice constant $a = 8.61$ Å are $A \equiv (0.25, 0.25, 0.25)$, $B \equiv (0.148, -0.148, 0.148)$, $C \equiv (0.078, -0.217, 0.0)$. The atoms C and C' and the other ten of the cage equivalent by symmetry are linked by an ethylenic-like bond 1.346 Å long [2,3].

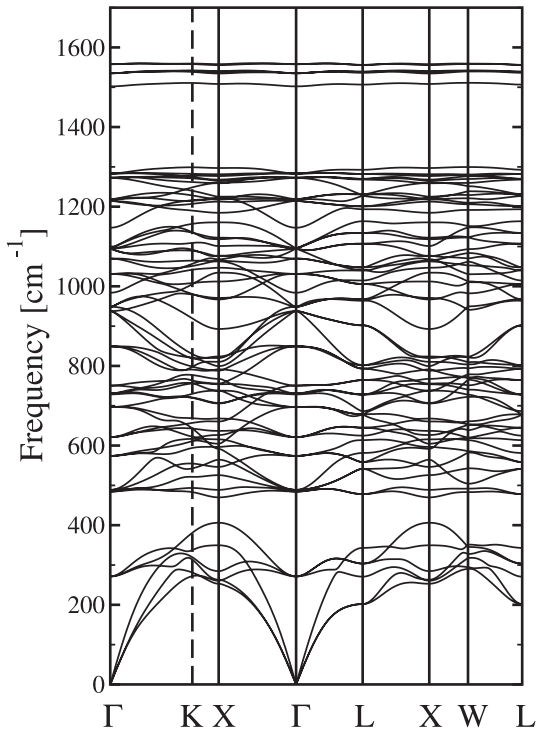

Fig. 2. Phonon dispersion relations of fcc-C_{22} along the high symmetry lines of the Brillouin Zone.

The effective charge tensor is finite for all atoms with maximum values in the off-diagonal components of atoms C (Fig. 1). This implies that the effective charge is mainly due to a charge transfer accompanying the bond modulation. The effective charge tensor for atoms A, B

Table 1. Symmetry and frequency of the Γ-point phonons of fcc-C_{22} (without LO-TO splittings).

Modes	Energy (cm^{-1})
$T_g(1)$	271
$E_g(1)$	484
$T_g(2)$	489
$T_u(1)$	574
$T_u(2)$	621
$T_g(3)$	697
$A_g(1)$	729
$T_u(3)$	731
$E_u(1)$	751
$T_g(4)$	849
$T_g(5)$	938
$T_u(4)$	949
$A_u(1)$	984
$T_u(5)$	1031
$E_g(2)$	1070
$T_g(6)$	1095
$T_u(6)$	1096
$A_g(2)$	1147
$E_u(2)$	1214
$T_g(7)$	1219
$A_u(2)$	1272
$T_u(7)$	1273
$T_g(8)$	1283
$A_g(3)$	1502
$T_u(8)$	1535
$E_g(3)$	1558

and C (Fig. 1) are given below in a.u.:

$$Z(A) = \begin{pmatrix} 0.230 & & \\ & 0.230 & \\ & & 0.230 \end{pmatrix}, \quad (2)$$

$$Z_{\alpha\beta}(B) = \frac{\partial P_\alpha}{\partial u_\beta} = \begin{pmatrix} b_1 & -b_3 & -b_2 \\ b_2 & b_1 & b_3 \\ b_3 & b_2 & b_1 \end{pmatrix}, \quad (3)$$

with $b_1 = 0.337$, $b_2 = -0.326$, $b_3 = 0.274$, P_α polarization, u_β atomic displacement and finally

$$Z(C) = \begin{pmatrix} -0.166 & 0.841 & \\ 0.267 & -0.235 & \\ & & -0.388 \end{pmatrix}. \quad (4)$$

The calculated dielectric constant is $\epsilon_\infty = 6.499$. From the phonon displacement pattern and effective charge tensors the IR spectrum shown in Figure 3 is obtained [11]. Due to the small effective charges and the large unit cell, the TO-LO splitting is small ($\lesssim 2$ cm^{-1}) except for the mode at 731 cm^{-1} ($T_u(3)$) which has a LO-TO splitting of 7 cm^{-1} (still hardly visible in Fig. 2). In fact, this latter mode corresponds to the strongest peak in the IR spectrum. Its displacement pattern is shown in Figure 4. The

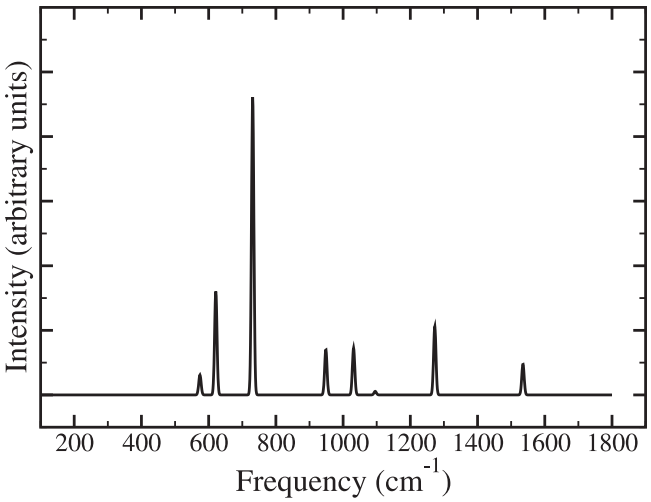

Fig. 3. Calculated IR spectrum of fcc-C_{22}.

Fig. 4. Displacement pattern of the Tu(3) mode of frequency of 731 cm^{-1} which gives the strongest peak in the IR spectrum (cf. Fig. 3 and Tab. 1).

Raman spectrum of fcc-C_{22} produced by the g modes in Table 1 has been reported in our previous work [2]. The IR spectrum of Figure 3 provides an additional fingerprint to be used to identify experimentally the fcc-C_{22} crystal.

4 Hydrogenated C_{20} polymers

The bco-C_{20} solid studied in references [2,4,9] is shown in Figure 5. The structure can be understood as obtained in two steps from C_{20} clusters arranged in an fcc lattice. First, in analogy with the tetragonal phase of polymeric C_{60} [10], polymeric planes of C_{20} are formed via [2+2] cycloaddition reaction along [110] and [$\bar{1}$10] directions of the fcc lattice (four [2+2] reactions per C_{20}, Fig. 5a). The 2D polymers stacked in the $ABAB$ sequence along [001] are further interlinked each other with eight additional intercluster bonds per C_{20}. We might envisage to cleave these latter interplanar bonds and stabilize the 2D polymer in a form similar to the tetragonal polymeric C_{60}. This can be achieved by saturating, at least partially, the eight dangling bonds per C_{20} arising from the separation of the polymeric planes. Partial hydrogenation by addition of four H atoms per C_{20} cluster allows to reach this goal. The new structure can also be seen as originated from [2+2] cycloaddition reactions of

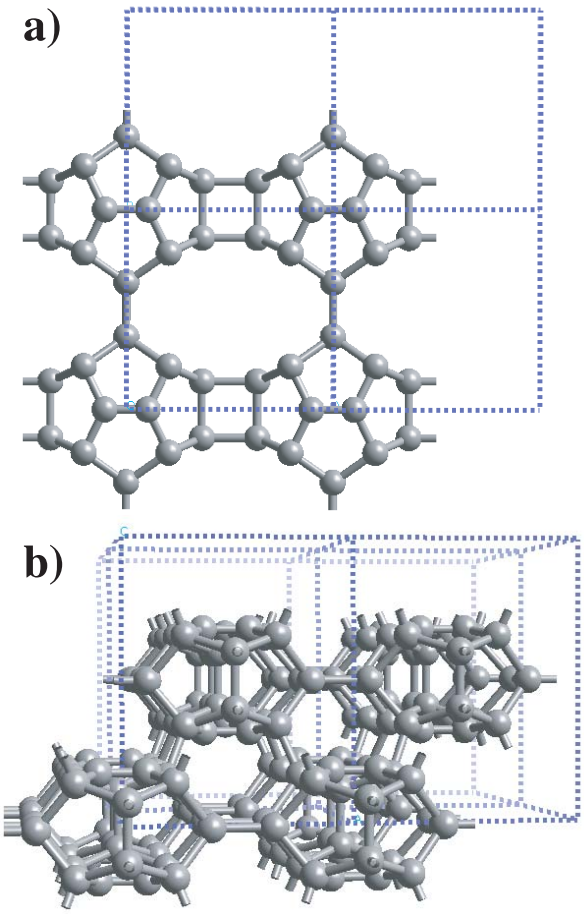

Fig. 5. Crystal structure of the bco-C_{20} solid (see text). (a) View of a single polymerized plane produced by four [2+2] cycloaddition reactions per C_{20} cluster. (b) View of the 3D bco-C_{20} crystal [2,4,9].

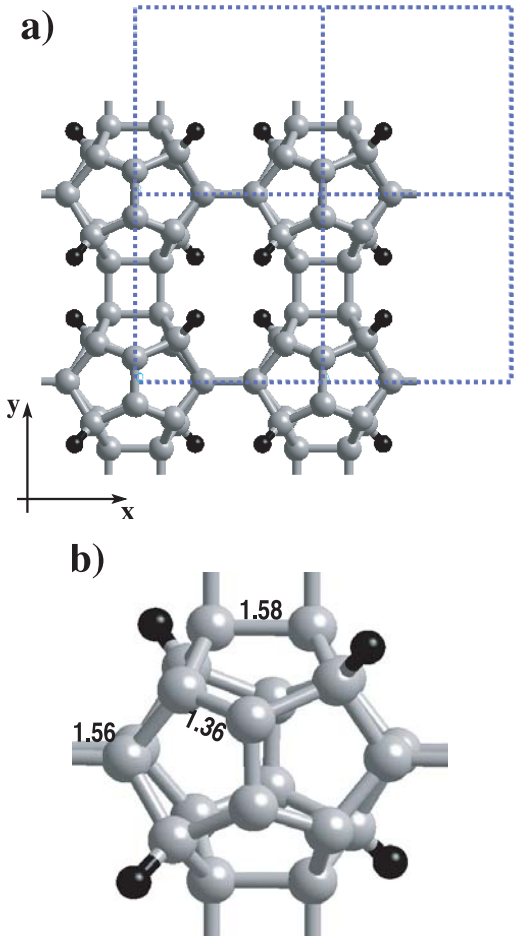

Fig. 6. a) Two-dimensional polymer of $C_{20}H_4$, obtained from isomer A (see text and Fig. 7). b) Geometry of the C_{20} unit inside the 2D polymer. The point group of the polymer is D_2. The lengths (in Å) of the double bonds and of the bonds taking part in the [2+2] cycloadditions are given (see text). Dark spheres indicate hydrogen atoms.

$C_{20}H_4$ precursors (Fig. 6). There are several isomers of the $C_{20}H_4$ fullerene differing in the position of the H atoms. Among them we have considered the isomers with H positions compatible with the formation of [2+2] cycloaddition reactions of bco-C_{20} as given in Figure 6. There are six clusters of this type obtained by inserting the hydrogen atoms on four positions among the eight dangling bonds per C_{20} produced by the cleavage of bco-C_{20} (Fig. 5). The structures and energies of the six clusters, named A, B, C, D, E and F are given in Figure 7 and Table 2. The calculations on the "isolated" clusters have been performed with 3D periodic boundary conditions in a cubic supercell with edge of 10.94 Å. These clusters might originate from partial dehydrogenation of the $C_{20}H_{20}$ molecule. The viability of this formation route might be supported by the calculation of the relative abundance of the $C_{20}H_n$ clusters as a function of the hydrogen number n. This analysis could reveal the presence of magic $C_{20}H_n$ clusters, but it is computationally very demanding due to the presence of a prohibitively large number of isomers and presently outside the scope of this work. The less symmetric clusters among those considered (E, F) have the lowest energies. However, the energy hierarchy is reversed when the 2D polymer is formed. In fact, the most symmetric isomer A gives rise to the polymer with the lowest energy (Fig. 6). The total energy of the 2D polymers formed by selected isomers are reported in Table 2. The internal structure and the a and b parameters of the 2D lattice have been fully optimized. In the optimization of the lattice parameters we have used a higher cutoff of 80 Ry to avoid the discontinuities due to the variation in the number of plane waves [17]. The calculation are performed with 3D periodic boundary conditions. The periodically repeated 2D polymers are separated by a vacuum 5 Å wide. The equilibrium lattice parameter for the most stable 2D polymer obtained from the isomer A (Fig. 6) are $a = b = 5.724$ Å. A large energy gain is found for the formation of intercluster bonds via the [2+2] cycloaddition reaction. The polymerization energy is ∼3 eV

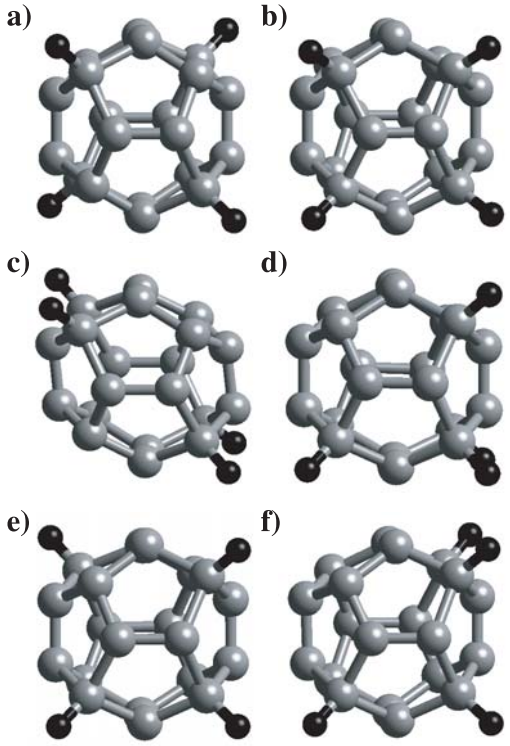

Fig. 7. Structure of six $C_{20}H_4$ clusters (see text). Panel (a) isomer A (D_2 point group symmetry), panel (b) isomer B (C_2), panel (c) isomer C (C_{2h}), panel (d) isomer D (C_1), panel (e) isomer E (C_1) and panel (f) isomer F (C_1).

Table 2. Total energies of the six $C_{20}H_4$ clusters (see text). The energy per C_{20} unit of the optimized 2D polymers of selected isomers is reported in the second column. The data correspond to calculations with an energy cutoff of 80 Ry (see text).

Cluster	Energy (eV)	Energy (eV)
A	1.035	–6.369
B	1.090	-
C	0.810	–6.212
D	1.020	-
E	0.068	–5.621
F	0.000	-

per [2+2] cycloaddition depending on the type of isomer (cf. Tab. 2). Note that this polymerization energy is much larger than that of the C_{60} polymer. In fact, the calculated polymerization energy of the tetragonal polymeric C_{60} is only 0.645 eV per [2+2] cycloaddition [18]. A sketch of the C_{20} unit of the most stable 2D polymer formed with isomer A is shown in Figure 6b. This latter polymer has D_2 point group symmetry. Four C-C bonds in the cluster (1.58−1.56 Å long) participate in the [2+2] cycloaddition reaction with neighboring clusters. Eight carbon atoms of the cluster form instead four C=C double bonds 1.36 Å long (Fig. 6b). The length of the other single C-C bonds in the cluster are in the range 1.43−1.59 Å while the inter-

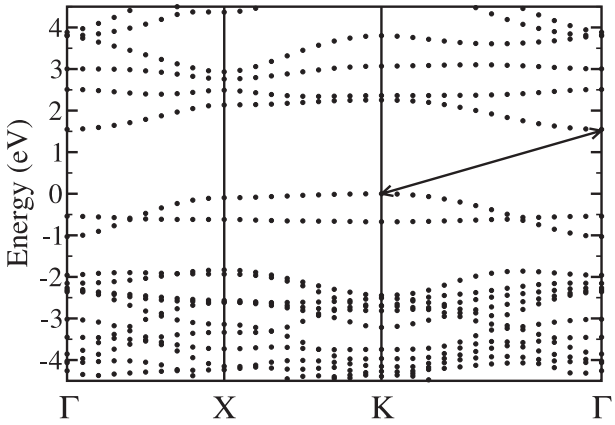

Fig. 8. Electronic band structure along the high symmetry directions of the 2D Brillouin Zone of polymeric $C_{20}H_4$ obtained from isomer A (see text and Fig. 6). Arrows indicate the indirect electronic band gap.

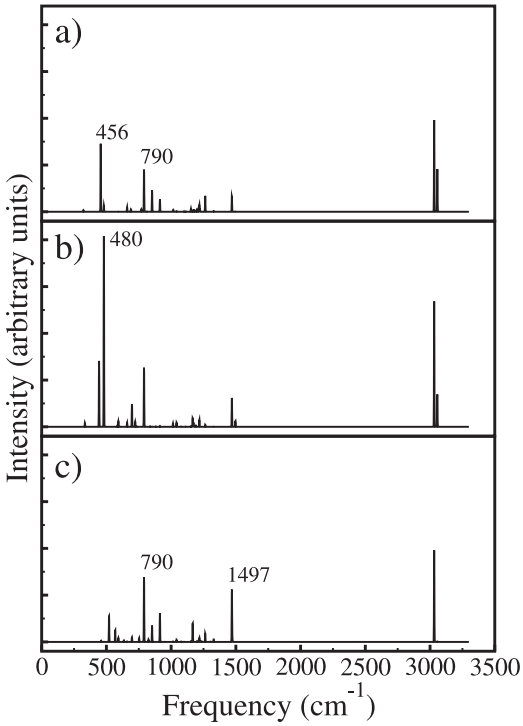

Fig. 9. Calculated Raman spectrum of 2D polymeric $C_{20}H_4$ (isomer A, see text and Fig. 6) in backscattering geometry along directions (a) x, (b) y, and (c) z with z perpendicular to the polymeric plane (cf. Fig. 6).

cluster bonds are 1.58 Å long. The electronic band structure along the high symmetry lines of the 2D Brillouin Zone is shown in Figure 8. The system is insulating with an indirect band gap of 1.55 eV. The uppermost valence bands and lowest conduction bands are very flat and originate from π bonding and π^* antibonding states of the C=C double bonds, respectively. The calculated Raman spectra in backscattering geometry of the 2D polymer (isomer A) are shown in Figure 9. We recognize four main peaks at 456, 480, 790 and 1497 cm^{-1}. The peak above

3000 cm^{-1} are due the CH stretching modes. The peak at 1497 cm^{-1} is a stretching mode of the C=C double bonds. The mode at 790 cm^{-1} is a quadrupolar deformation of the cluster cage along the axis connecting two hydrogen atoms above and below the polymeric plane. The peaks at 456 and 480 cm^{-1} are stretching and bending modes of the bonds involved in the [2+2] cycloaddition. The Raman spectra of the other 2D polymers formed by isomers E and C similarly show four strongest peaks at frequencies slightly different from those of isomer A (within 30 cm^{-1}) but with very similar displacement patterns. These features could be used as fingerprints of the $C_{20}H_4$ polymers in the experimental search for C_{20}-based solids.

5 Conclusion

In summary, we have computed the phonon dispersion relations and IR spectrum of the *fcc*-C_{22} crystal, recently proposed in a joint experimental and theoretical report [2]. Our calculations provide further data which would aid the compelling experimental identification of this new carbon phase. Other possible competitive structures made by assembling C_{20} clusters have been considered in literature [2,4]. Here, we have studied the geometry and Raman spectra of two-dimensional polymers made from [2+2] cycloaddition reactions of $C_{20}H_4$ clusters. Although these polymeric forms are only theoretical structures at the moment, one might envisage to synthesize these phases by deposition of partially hydrogenated C_{20} clusters on a metallic substrate at low coverage. One might speculate that the high reactivity of the C_{20} clusters would promote their condensation into polymers [19] and that the partial hydrogenation might stabilize a polymeric plane with respect to the 3D network of the *fcc*-C_{22} phase, found experimentally under the deposition conditions of reference [2]. Supersonic cluster beam deposition has been recently proven to be an efficient tool for the deposition of carbon films with a controlled nanostructures [20,21]. The combination of this technique with the above-mentioned methods [1,2] for the production of stabilized C_{20} cages in the gas phase is suggested as a possible route for the production of (hydrogenated) C_{20} polymer films on suitable substrates.

This work is partially supported by MURST through project PRIN01-2001021133 and by the INFM Parallel Computing Initiative.

References

1. H. Prinzbach, A. Weiler, P. Landenberger, F. Wahl, J. Wörth, L.T. Scott, M. Gelmont, D. Olevano, B.V. Issendorff, Nature **407**, 60 (2000)
2. Z. Iqbal et al., Eur. Phys. J. B **31**, 509 (2003)
3. I. Spagnolatti, M. Bernasconi, G. Benedek, Europhys. Lett. **59**, 572 (2002)
4. S. Okada, Y. Miyamoto, M. Saito, Phys. Rev. B **64**, 245 (2001)
5. J.C. Grossman, S.G. Louie, M.L. Cohen, Phys. Rev. B **60**, R6941 (1999)
6. N. Breda, R.A. Broglia, G. Colò, G. Onida, D. Provasi, E. Vigezzi, Phys. Rev. B **62**, 130 (2000)
7. A. Devos, M. Lannoo, Phys. Rev. B **58**, 8236 (1998)
8. As an addition to the discussion of reference [3] we here report that the insertion of Na in the fcc-C_{22} solid from the vapor phase of Na_2 molecules is an exhothermic reaction, the calculated difference in energy being 0.49 eV per Na atom
9. A. Mussi, Undergraduate Thesis in Physics, Department of Physics, University of Milano, 2001, unpublished
10. M. Núñez-Regueiro et al., in *Fullerene Polymers and Fullerene Polymers Composites*, edited by P.C. Eklund, A.M. Rao (Springer-Verlag, Berlin, 2000)
11. S. Baroni, S. de Gironcoli, A. Dal Corso, P. Giannozzi, Rev. Mod. Phys. **73**, 515 (2001)
12. We used the PWSCF and PHONON codes developed by S. Baroni, P. Giannozzi, S. de Gironcoli, A. Dal Corso and others [11]: `http://www.pwscf.org`
13. H.J. Monkhorst, J.D. Pack, Phys. Rev. B **13**, 5188 (1976)
14. R. Car, M. Parrinello, Phys. Rev. Lett. **55**, 2471 (1985)
15. CPMD V3.5 Copyright IBM Corp 1990-2003, Copyright MPI fuer Festkoerperforschung Stuttgart 1997-2003
16. J. Martin, S. Montero, J. Chem. Phys. **80**, 4610 (1984)
17. G. Francis, M. Payne, J. Phys. Condens. Matt. **2**, 4395 (1990)
18. S. Okada, S. Saito, Phys. Rev. B **59**, 1930 (1999)
19. A.J. Du, Z.Y. Pan, Y.K. Ho, Z. Huang, Z.X. Zhang, Phys. Rev. B **66**, 35405 (2002)
20. D. Donadio, L. Colombo, P. Milani, G. Benedek, Phys. Rev. Lett. **83**, 776 (1999)
21. E. Barborini et al., Appl. Phys. Lett. **81**, 3359 (2002)